Molecular Biology of the Cell
Vol. 7, 443–455, March 1996

Juvenile and Mature MAP2 Isoforms Induce Distinct Patterns of Process Outgrowth

Nicole Leclerc,* Peter W. Baas,† Craig C. Garner,‡ and Kenneth S. Kosik§¶

*Département de Pathologie, Université de Montréal, Québec H3C 3J7, Canada; †Department of Anatomy, University of Wisconsin Medical School, Madison, Wisconsin 53706; ‡Department of Anatomy and Cell Biology, University of Alabama at Birmingham, Birmingham, Alabama 35294; and §Harvard Medical School and Center for Neurologic Diseases, Department of Medicine (Division of Neurology), Brigham and Women's Hospital, Boston, Massachusetts 02115

Submitted September 15, 1995; Accepted December 15, 1995
Monitoring Editor: Martin Raff

Microtubule-associated protein-2 (MAP2) is the most abundant MAP in neurons, where its distribution is restricted to the somatodendritic compartment. This molecule undergoes developmentally regulated alternative splicing, resulting in at least two isoforms, a juvenile isoform (termed MAP2c) and a mature isoform (MAP2), with greatly different molecular masses. Spodoptera frugiperda (Sf9) cell expression of the juvenile versus the mature MAP2 isoform generates two distinct patterns of process outgrowth. The smaller juvenile isoform induces multiple short thin processes. Mature MAP2 tends to induce single processes that are considerably thicker than those processes induced by juvenile MAP2. We found important differences in the variability of spacing between microtubules and the number of microtubules along the processes induced by MAP2c and mature MAP2. MAP2c showed variability with most microtubules spaced as closely as with tau, but some spaced as far apart as with mature MAP2. Over their length, the mature MAP2 processes demonstrate proximo-distal taper, which corresponds to a narrowing of the spacing between microtubules from 90 nm to 40 nm. Moreover, there is a decreased number of microtubules in mature MAP2-induced processes whereas in tau and MAP2c-induced processes, the number of microtubules is constant along the length. Based on these observations, we conclude that MAP2 isoforms can serve as architectural elements by establishing specific morphological features of processes and specific arrangements of their microtubules.

INTRODUCTION

The problem of how cytoskeletal proteins assemble and interact with membranous elements to establish their unique shapes is particularly evident in neurons, which generally establish two distinct compartments: the axon and the dendrite. Most neurons generate a single axon that is uniform in diameter and grows over exceedingly long distances. In contrast, dendrites are usually multiple in number, significantly shorter, broad in caliber, and taper with distance from the cell body (Bartlett and Banker, 1984; Hillman, 1988). Marking the differentiation of dendrites and axons are two populations of microtubules with distinct organizations. In the axon, microtubules are relatively closely spaced and are oriented with their plus ends distal to the cell body, whereas dendritic microtubules are spaced farther apart and are oriented in both directions (Heidemann *et al.*, 1981; Baas *et al.*, 1988; Burton and Paige, 1981). The spacing and orientation of microtubules may have profound implications with regard to the growth properties of neurites and their capacity to accommodate the transport of different types of cytoplasmic organelles.

Other than spacing and polarity orientation, the most profound difference between axonal and dendritic microtubules appears to be compositional. Mi-

¶ Corresponding author: LMRC-Brigham and Women's Hospital, 221 Longwood Ave, Boston, MA 02115.

crotubules within living cells are decorated with a class of proteins termed microtubule-associated proteins (MAPs) that regulate features of their assembly, stability, rigidity, and interaction with neighboring microtubules and other structures within the cytoplasm. Microtubules in the neuron are fundamentally important for the differentiation, growth, and maintenance of axonal and dendritic processes. The most pronounced differences of the MAP composition between axons and dendrites is that tau is highly enriched in axons while MAP-2 is absent from the axon and enriched within the dendrite (reviewed in Kosik and Caceres, 1991). The segregation of cytoskeletal proteins appears to play a crucial role in the generation and/or maintenance of morphologically and biochemically distinct dendritic and axonal compartments. It has been clearly demonstrated that MAPs, in particular MAP2 and tau specifically expressed in neurons, are pivotal molecules for the production of dendritic and axonal processes. After initial formation of exploratory neurites, one of these becomes an axon and the others differentiate into dendrites (Banker and Goslin, 1990). The suppression of MAP2 expression inhibits the development of the exploratory neurites whereas that of tau prevents the differentiation and maintenance of the axonal process (Caceres and Kosik, 1990; Caceres *et al.*, 1991, 1992). Based on these observations, it may be concluded that MAP2 is required at an earlier stage of neuronal morphogenesis than tau. Later on, MAP2 expression is necessary to maintain dendrites (Sharma *et al.*, 1994). To date, the molecular interactions underlying the function of MAP2 as a determinant of the distinctive morphology of a neuron remain only partially understood.

MAP-2 is a complex molecule that exists in multiple isoforms whose expression and appearance are under developmental regulation. To fully appreciate the role of MAP2 in cellular morphogenesis, it becomes crucial to elucidate the functional differences among isoforms. MAP2 consists of a microtubule-binding domain at the carboxy terminus and a long projection domain within which a developmentally regulated splicing event (Garner and Matus, 1988) introduces 1372 amino acids (Papandrikopoulou *et al.*, 1989; Kindler, *et al.*, 1990). This splicing event shifts the apparent molecular mass of MAP2 on SDS-PAGE from a ~70-kDa juvenile form (termed MAP2c) to a ~280-kDa mature form. Initially during neuronal differentiation, both MAP2c and the mature form of MAP2, termed MAP-2b, are expressed. The former is referred to as mature MAP-2 because it persists throughout the life of the neuron, while the latter is referred to as juvenile MAP-2 because it diminishes during development (Ludin and Matus, 1993). As MAP2c disappears, it is replaced by MAP-2a, another mature isoform with a slightly different electrophoretic mobility compared with MAP-2b. MAP-2a and MAP2b are found exclusively in dendrites while MAP2c is found in both dendrites and axon (Ludin and Matus, 1993). MAP-2 shares a high sequence homology with tau in the carboxyl-terminal, but the molecules are also very different in the projection domain (Lewis *et al.*, 1988).

To understand how each of the MAP2 isoforms contributes to the elaboration of the neuronal morphogenesis sequence, it is necessary to individually express the isoforms in a system where they exert morphological effects. The infection of normally rounded insect ovarian Sf9 cells with a virus containing a tau and a MAP2 cDNA insert results not only in promoting microtubule assembly, stabilization, and bundling, but also in inducing the formation of processes (reviewed in Kosik and McConlogue, 1994). The expression of the axonal MAP, tau, in nonneuronal Sf9 cells, induced the formation of a single long process of uniform caliber (Knops *et al.*, 1991). Like tau expression, the expression of mature MAP-2 and MAP2c induces the cells to extend microtubule-rich processes (Chen *el al.*, 1992; Leclerc *et al.*, 1993). The microtubules within tau-, mature MAP-2-, and MAP2c-induced processes are uniformly plus-end-distal, indicating that the differences in microtubule polarity orientation between axons and dendrites cannot be explained by differences in MAP composition, at least not directly (Baas *et al.*, 1991; Chen *et al.*, 1992; Leclerc *et al.*, 1993). However, spacing between microtubules is greater for adult MAP-2 than for tau, as is the spacing between microtubules in dendrites compared with axons (Chen *et al.*, 1992). The spacing between microtubules in MAP2c-induced processes was similar to that of tau. Also, the expression of FS, a MAP2c-like construct, in which 109 amino acids had been deleted from the region that flanks the microtubule-binding domain, induced a spacing similar to MAP2c (Leclerc *et al.*, 1993). Based on these results, it was concluded that the projection domain determines the spacing between microtubules. The consequences of the distinct MAP regulation of microtubule organization in living cells, and ultimately on process morphology and outgrowth, is still poorly understood.

In this study, we focused on the differential effects of mature MAP-2 and MAP-2c on process morphology and outgrowth. To do so, we provide a quantitative analysis of the process morphology, focusing on process number, length, and caliber. MAP2c has a higher tendency than FS to induce multiple processes whereas mature MAP2 induces single process. Our results therefore suggest a role for the projection domain in setting up the number of processes. We also demonstrated differences in caliber. Mature MAP2 processes are short, thick, and taper whereas MAP2c induced thin processes of uniform caliber similar to FS- and tau-induced processes. To better understand how MAPs may determine process caliber, we examined the spacing and number of microtubules along

the length of the process. We observed a decrease in both spacing and microtubule number concomittant with the decrease in caliber along mature MAP2 processes. In MAP2c- and tau-induced processes, the spacing remains constant along the process.

MATERIALS AND METHODS

Baculoviral Recombinants

Full-length rat MAP2c and full-length mouse mature MAP2 cDNAs were cloned into the baculovirus transfer vector pVL1392 (Invitrogen, San Diego, CA). The rat MAP2c sequence cloned in the PCMVN vector was digested with *Not*I and cloned into the *Not*I of the transfer/expression vector pVL1392. The mature MAP2 sequence cloned in the PSV vector was digested with *Sal*I and *Ase*I, filled in with Klenow, linked with *Bcl*I linkers, and subcloned into the *Bam*HI site of the Bluesript SKII+ vector (Stratagene, La Jolla, CA). The MAP2 sequence was cut out of the BlueScript SKII+ vector by digestion with *Cla*I, filled in with Klenow, and then digested with *Not*I. The MAP2 insert was assembled into the *Not*I and *Sma*I of the baculovirus expression vector, pVL 1392. The MAP2c and mature MAP2 sequences were inserted into the genome of the *Autographa californica Multiple Nuclear Polyhedrosis Virus* (AcMNPV) by homologous recombination (Summers and Smith, 1987). The transfer vector containing MAP2c or MAP2 sequence was cotransfected with a modified form of the baculovirus, AcMNPV, designated AcRP6-SC (Invitrogen), onto the Spodoptera frugigerpa (Sf9) cells using the lipofectin procedure (Life Technologies, Grand Island, NY). AcRP6-SC viral DNA was linearized by digestion with endonuclease *Bsu 36I* (Kitts *et al.*, 1990). Viral DNA (1 μg) and transfer vector (5 μg) were used to transfect the Sf9 cells. The Sf9 cells were obtained from the American Type Culture Collection (ATCC #CRL 1711; Rockville, MD) and were used to propagate wild-type and recombinant baculoviruses. Sf9 cells were grown in suspension or as a monolayer at 27°C in Grace's medium (Life Technologies) supplemented with 10% (vol/vol) fetal bovine serum (JRH Biosciences, Lenexa, KS). After 48 h at 27°C, the transfection supernatant was purified by a standard plaque assay for occlusion-body-negative recombinant viral plaques and by limiting dilution (Fung *et al.*, 1988). The recombinant virus was amplified to yield titers of 10^8-10^9 plaque-forming units/milliliter.

Sf9 Cell Expression

For immunocytochemistry the cells were fixed in 3.7% paraformaldehyde in phosphate-buffered saline (PBS) and 0.12 M sucrose at 48 and 72 h post-infection and then extracted in .3% Triton X-100 in PBS for 5 min. The fixed cells were labeled with the monclonal antibody, AP18 (kindly provided by Dr. L. Binder; Tucker *et al.*, 1988) directed against both MAP2c and mature MAP2, 46.1 (kindly provided by Dr. Virginia Lee) or 5E2 (Kosik *et al.*, 1988), two monoclonal antibodies directed against tau and anti-α-tubulin antibody (clone DM 1A; Sigma, St. Louis, MO). After blocking with 10% normal horse serum in PBS, the cells were incubated in the primary antibody overnight at 4°C, washed three times in PBS, incubated with a goat anti-mouse fluorescein isothiocyanate-conjugated antibody for 40 min at 37°C, washed in PBS, mounted in polyvinyl alcohol mounting media, and visualized by fluorescence microscopy.

The expression of MAP2c or mature MAP2 recombinant protein was confirmed by immunoblot analysis using the monoclonal antibody AP18. The anti-tau antibody, 46.1 or 5E2, was used to confirm the presence of tau protein. The cells were scraped in Laemmli buffer and boiled for 5 min. The sample were separated on an 8% polyacrylamide gel. Proteins were electrophoretically transferred to nitrocellulose filters as described by Towbin *et al.* (1979) and analyzed on an immunoblot. Heat-stable MAPs were prepared by sonicating cells in 0.1 M MES, pH 6.4, 1 mM EGTA, and 0.5 mM $MgCl_2$, spinning at 1000 $\times$ *g* for 10 min at 4°C. The low-speed supernatant was adjusted to 0.75 M NaCl and 2% 2-mercaptoethanol and boiled for 10 min, and then centrifuged at 200,000 $\times$ *g* for 30 min at 4°C. The protein determinations were done by the Bio-Rad protein detection system (Richmond, CA). The supernatant was gel electrophoresed. To minimize quantitative differences in the level of expression of each MAP isoform, the constructs were driven by the same polyhedrin promoter, and the multiplicity of infection was identical. For comparisons with tau-induced processes, a baculovirus containing the three-repeat tau isoform was used as previously reported (Knops *et al.*, 1991).

Morphometry

Processes from three sets of 50 cells each were counted and used to calculate the mean and standard errors (M $\pm$ SD). The statistical significance was determined using a two-tailed Student's *t* test. Statistical significance was accepted if $p < 0.05$. The caliber was measured at five equally spaced points along each process ($n = 35$ for each construct).

The image obtained from a Nikon Diaphot-TMD inverted microscope was projected to a Hamamatsu video camera and displayed on a DAGE-MTI multi-scan high resolution monitor. Images were analyzed by the Image I software (Universal Imaging, West Chester, PA).

Electron Microscopy

For transmission electron microscopy, Sf9 cells were grown in 35-mm tissue culture dishes at a density of 10^6 cells. The cultures were fixed in 2% glutaraldehyde for 10 min, rinsed in a solution containing 0.1 M cacodylate and 5% sucrose, stained with 2 mg/ml tannic acid for 5 min, rinsed again, postfixed for 5 min with 1% osmium tetroxide, dehydrated with increasing concentrations of ethanol, and embedded using Quetol 653 resin (Ted Pella, CA).

After curing the resin, cells of interest were located by phase-contrast microscopy, circled with a diamond marker objective, and sectioned either parallel or perpendicular to the long axis of the processes (Baas and Heidemann, 1986; Baas *et al.*, 1987)

RESULTS

Expression of MAP2 Isoforms in Sf9 Cells

Spodoptera frugiperda (Sf9) cells were infected with baculovirus recombinants containing MAP2c or mature MAP2. For comparison with tau expression, we used a baculovirus containing the three repeat tau isoform (Knops *et al.*, 1991). At a mutiplicity of infection of 5, the onset of recombinant protein expression became detectable 20 h after the addition of virus to the medium, a time coincident with process formation (Knops *et al.* 1991; Knowles *et al.* 1994). By 48 h post-infection, nearly 60% of the cells expressing MAP2c and approximately 20% of the cells expressing mature MAP2 had processes, and all of these were reactive with the MAP2 antibody AP18. To confirm the expression of MAP2c, mature MAP2, and tau recombinant protein, the cells were scraped in boiling sample buffer, loaded on SDS-PAGE, and analyzed by immunoblotting. Immunoblot analysis using AP18, a monoclonal antibody directed against a common epitope to the low and high molecular weight MAP2 isoforms, revealed a band of 68 kDa or 280 kDa when prepared

from cells expressing MAP2c and mature MAP2, respectively (Figure 1A). No AP18 immunostaining was detectable in noninfected cells or in cells infected with wild-type virus. By using an anti-tau antibody, tau appeared as at least two bands (Figure 1A). Frequently the MAP2c and tau signal appeared as a closely spaced doublet, suggesting that post-translational modification might occur in the Sf9 cells.

Further confirmation of MAP expression within the infected cells was derived from studies showing that after heat treatment (to which MAP2 and tau are stable), the major protein on Coomassie-stained gels was the specific MAP expressed whereas in wild-type–infected cells, only very faint bands of protein were detectable (Figure 1B). The level of expression of MAP2c, mature MAP2, and tau recombinant protein was measured after heat treatment and was compared with the amount of heat-stable protein in wild-type–infected cells at different times post-infection.

The quantification of protein expression was performed to determine at what time post-infection MAP2c, mature MAP2, and tau expression is at identical molar ratios. The expression of MAP2c (~4.8 μg) and mature MAP2 (~24 μg) is at an identical molar ratio at approximately 24 h post-infection for MAP2c and 72 h post-infection for mature MAP2. Although tau (~4 μg) was at an identical molar ratio with MAP2c and mature MAP2 at 24 h post-infection, its expression was higher than MAP2c and mature MAP2 at 36 and 72 h post-infection (Figure 1B).

At 24 h post-infection, some MAP2c-expressing cells had already developed multiple processes (Figure 2A). At 36 h post-infection, many cells clearly had the tendency to develop multiple processes (Figure 2B). Mature MAP2-expressing cells began to form processes at 48 h post-infection (Figure 2C). They usually had one process. Approximately 30% of the cells expressing mature MAP2 developed processes at 72 h post-infection (Figure 2D). As previously observed, tau-expressing cells initiated process outgrowth at 24 h post-infection (Figure 2E). At any time of infection, they generally presented one process (Figure 2F). Tubulin expression levels in the case of the tau construct were unchanged relative to infection with the wild-type baculovirus (Cheley *et al.*, 1992), consistent with the known tendency of the baculovirus to suppress transcription.

As revealed by an anti-tubulin antibody, the microtubule distribution in mature MAP2-expressing cells differed from that of MAP2c-expressing cells. At 24 h post-infection in MAP2c-expressing cells that presented multiple processes, the microtubule bundles emerged radially or tangentially from the cell surface to form processes as noted at later stages of infection (Figure 3, D and E). In the immunoreactive cells that did not have processes, the tubulin staining was diffusely distributed in the cytoplasm (Figure 3D). At 36–48 h post-infection, in some cases, bundles of microtubules were oriented in one direction, and joined together at one pole of the cell to form a single process (Figure 3F). At 48 h post-infection, mature MAP2 expression did induce microtubule assembly. In the MAP2-immunoreactive cells that did not develop processes, the microtubules were distributed in rings under the plasma membrane (Figure 3A). In the cells that initiated process outgrowth, the microtubules joined

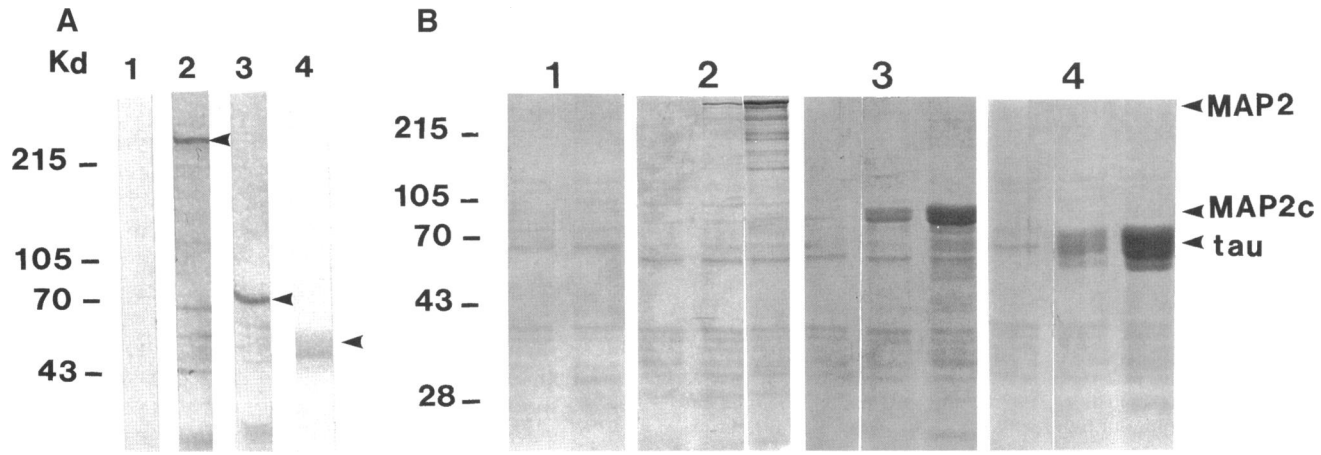

Figure 1. (A) Immunoblot of baculoviral-expressed mature MAP2 (lane 2), MAP2c (lane 3), and tau (lane 4) harvested 72 h after infection. The samples were run on 6% SDS-PAGE and immunoblotted with antibody AP18 (anti-MAP2) and antibody 46.1 (anti-tau). There was absence of antibody reactivity with endogenous protein in wild-type–infected Sf9 cells (lane 1). Molecular mass standards are indicated on the left: ovalbumin (43 kDa), bovine serum albumin (70 kDa), phosphorylase b (105 kDa), myosin (215 kDa). (B) Time course of mature MAP2, MAP2c, and tau expression in Sf9 cells. There was ~8 μg, 9.2 μg, and 24 μg of mature MAP2; ~4.8 μg, 9.6 μg, and 28.8 μg of MAP2c protein; and ~4 μg, 17.6 μg, and 43.2 μg of tau protein in 10^6 cells at 24, 36, and 72 h post-infection, respectively. Lane 1 represents heat-stable proteins in wild-type–infected cells harvested at 36 and 72 h after infection, respectively.

in the hillock region to form a single process. This was more evident at 72 h post-infection (Figure 3B), and in certain cases, microtubules formed a single bundle in the cell body (Figure 3C). Most of the mature MAP2-expressing cells contained microtubule bundles, indicating that the relatively lower percentage of processes on these cells was not due to failure of microtubule assembly. Collectively, these data demonstrate that the expression of a particular MAP determines successful process elaboration, and suggest that microtubule assembly alone is an insufficient determinant of process formation.

Quantitative Comparison of Process Morphologies Induced by MAP2 Isoforms

Both mature MAP2 and MAP2c induced processes, however, the morphologies of the processes differed from each other and from tau-induced processes. The morphological analysis was performed on unfixed cells because the cells had the tendency to detach and the very thin processes were lost during the fixation procedure. Process morphology was quantitated according to three parameters: process number, length, and caliber at 72 h post-infection. These data are summarized in Table 1. As shown by histograms of the

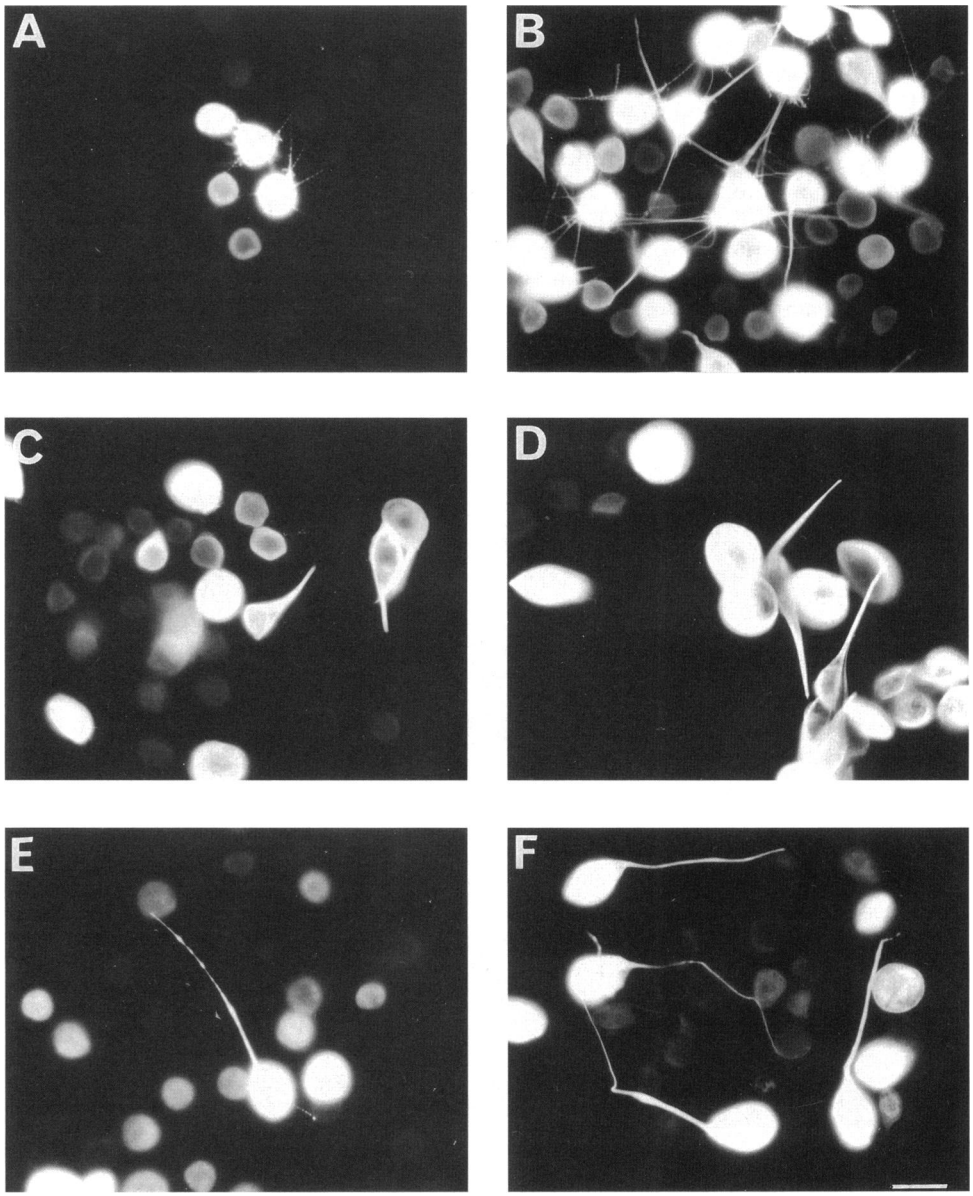

Figure 2. Immunofluorescence micrographs showing the process morphologies induced in Sf9 cells: MAP2c induces multiple processes at 24 h (A) and 36 h post-infection (B); mature MAP2 induces short tapered process at 48 h (C) and 72 h post-infection (D); and tau protein induces a long solitary process at 24 h (E) and 36 h (F) post-infection. Cells were stained with either monoclonal antibody AP18 against MAP2 or 46.1 against tau. Bar, 20 μm.

Table 1. Comparative analysis of process morphologies resulting from the expression of mature MAP2, MAP2c, and tau in SF9 insect cells

Construct	Number of Processes				Total process length (μm)	Process length (μm)	Process width (μm)	
	1	2	3	>3			Proximal	Distal
MAP2	29.67 ± 2.91	10.67 ± 2.91	4.0 ± 0.0	5.33 ± 2.60	60.42 ± 2.53	31.03 ± 1.19	4.59 ± 0.2	1.6 ± 0.1
MAP2c	13.33 ± 2.03	8.0 ± 1.53	.67 ± .67	27.67 ± 1.76	141.36 ± 6.45	26.22 ± .97	1.2 ± 0.1	1.0 ± 0.0
tau	35.67 ± 1.45	9.6 ± 1.45	2.0 ± .58	2.33 ± .88	122.37 ± 6.45	84.59 ± 4.22	2.0 ± 0.1	1.3 ± 0.1

For each determination three sets of 50 cells were counted. All values are the mean ± SEM.

number of processes per cell, MAP2c induced the greatest number of processes, whereas tau and mature MAP2 tended to induce single processes (Figure 4). Counts of groups of 50 process-bearing cells for MAP2c revealed that MAP2c had the highest percentage of cells with more than three processes, with ~60% compared with ~5% and ~10% for tau and mature MAP2. Some MAP2c-expressing cells had as many as 20 processes. In contrast, tau and mature MAP2 demonstrated a higher tendency to induce one process, with ~70% and ~60% of the cells, respectively, having a single process; for MAP2c, 27% of the cells presented one process. Control infections with wild-type baculovirus and viral recombinants expressing unrelated proteins had no effect on the morphology of the Sf9 cells.

Each of the MAPs expressed here could also be distinguished in terms of process length. Mature MAP2 generally induced relatively short processes (31.0 ± 1.2 μm). MAP2c also had short processes (26.2 ± 1.0 μm), but because this isoform tended to induce multiple processes, the mean summed length of all the processes was 141.4 ± 6.5 μm for MAP2c, compared with 60.4 ± 2.5 μm for mature MAP2. The total summed lengths of the processes per cell did not significantly differ between MAP2c and tau; however, the mean length of each process was shorter for the processes induced by MAP2c. The total summed lengths of the processes and the mean length of each process did significantly differ between MAP2 and tau. MAP2-induced processes were shorter than tau-induced processes.

The caliber of processes induced by mature MAP2 differed from cells expressing MAP2c or tau by their tendency to taper as measured by a series of points along the process (Figure 5). The mean width of pro-

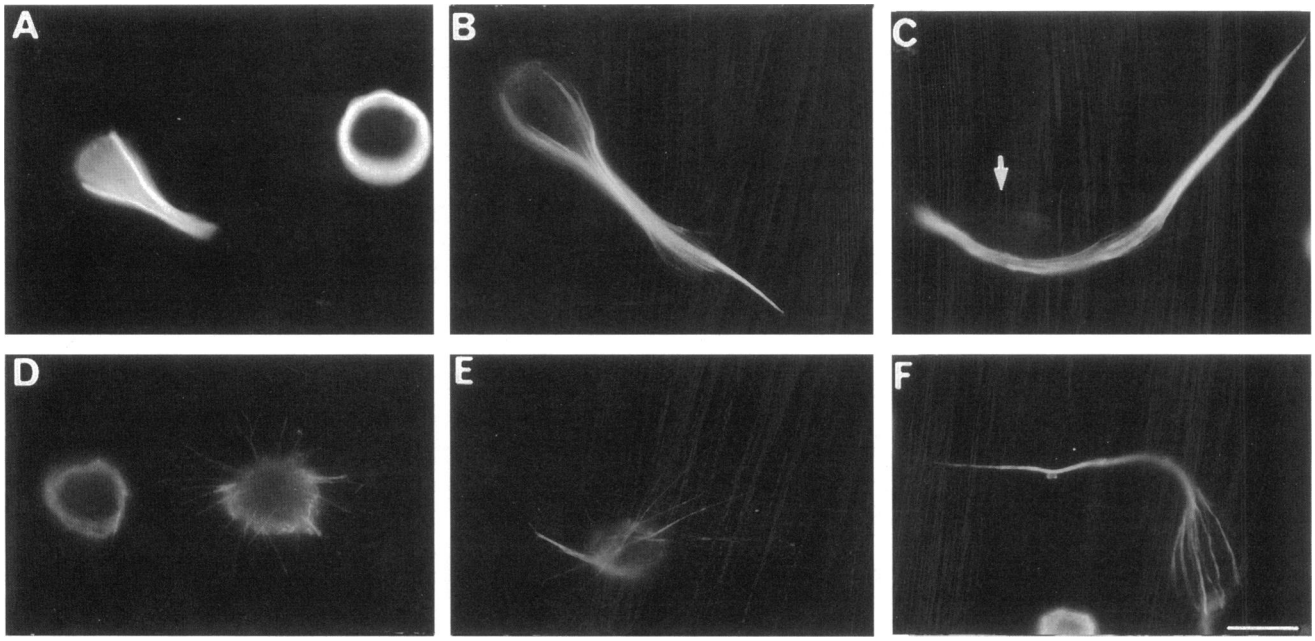

Figure 3. Microtubule bundles induced by mature MAP2 and MAP2c in Sf9 cells. Mature MAP2-expressing cells stained for tubulin with a monoclonal antibody to α-tubulin (clone DM 1A; Sigma) at 48 h (A) and 72 h post-infection (B and C), and MAP2c-expressing cells stained for tubulin at 24 h post-infection (D) and 36 h post-infection (E and F). Bar, 20 μm.

cesses induced by mature MAP2 was significantly greater at proximal points than at distal points. Proximally the mean width was 4.59 ± 0.2 μm, and distally it narrowed to 1.6 ± 0.1 μm. Comparable proximal and distal distances for MAP2c-induced processes were 1.2 +/0.1 μm and 1.0 ± 0.0 μm, and for tau-induced processes, 2.0 ± 0.1 μm and 1.3 ± 0.1 μm. These latter processes were somewhat broader in the few microns nearest the cell body, but usually did not exceed 2 μm even in this region. Rare cells expressing MAPs other than mature MAP2 had processes that tapered, and a few cells expressing mature MAP2 had processes that did not taper. Shared among all processes that tapered regardless of the expressed MAP was a thick (greater than 3 μm) initial segment. This observation suggested that any process beginning with an initial segment of a certain thickness would taper, and that mature MAP2 tended to induce this type of process with a much higher significant probability than other MAPs.

Microtubule Spacing in MAP2-induced Processes

We examined the spacing of microtubules along the processes induced by MAP2c and mature MAP2. In previous studies, it was determined that the average spacing between microtubules in tau-induced processes, FS-induced processes, and MAP2c-induced processes is about 20 nm, but is over 60 nm in processes induced by mature MAP2 (Baas *et al.*, 1991; Chen *et al.*, 1992; Leclerc *et al.*, 1993). Our present results confirm these previous findings, but indicate that the issue of microtubule spacing is more complex. With tau and FS, the variability in microtubule spacing was low (as reflected by a relatively modest standard deviation), and was not a function of position along the process. More careful analyses indicated important differences in the variability of spacing between microtubules among the processes induced by MAP2c and mature MAP2. Given that serial reconstruction of cross-sections is extremely time consuming, we analyzed only a single process induced by each of the MAPs (Figure 6) and we documented more extensively the microtubule spacing variability along processes by analyzing three additional MAP2c- and MAP2-induced processes in longitudinal sections (Figure 7). We measured the wall-to-wall spacing between neighboring microtubules at 50 randomly selected points between microtubules in the proximal, the middle, and the distal portion of three MAP2c and mature MAP2-induced processes.

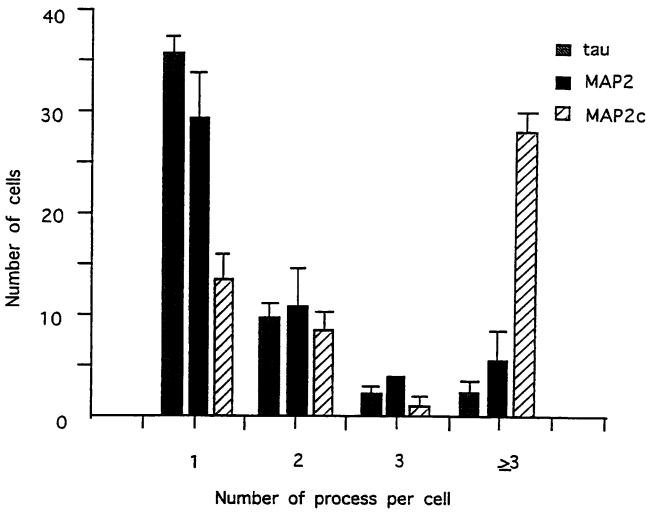

Figure 4. Histogram of the number of processes per cell induced by tau, mature MAP2, and MAP2c in Sf9 cells. See RESULTS for details.

Electron micrographs illustrated the proximodistal taper decrease in diameter of cross sections taken approximately 10 μm apart in a MAP2-induced process (Figure 6A). We measured the spacing and the cross-sectional number of microtubules. The spacing between adjacent microtubules varied for mature MAP2, but this variability was orderly, with microtubules getting progressively closer with distance from the cell body (Figure 6B). At similar intervals of 10 μm, the average spacing between microtubules was 90 ± 30.0, 70.9 ± 27.6, 60.2 ± 20.1, and 42.1 ± 18.0 nm (Figure 6D). In parallel studies on MAP2c, the average spacing between microtubules remained constant at 20–30 nm along the length of the process (Figure 6D). Furthermore, the microtubule number decreased as a function of distance along the process: moving distally from the cell body at 10-μm intervals, the number of microtubules was 556, 450, 263, and 110 (Figure 6C). In MAP2c and tau processes, the number of microtubules remained more consistent along the process (Figure 6C).

Given the technical complexity of serial cross-sectioning, we further examined the spacing between microtubules using longitudinal sections. MAP2c showed far more variability, with most microtubules spaced as closely as with tau (Baas *et al.* 1991; Chen *et al.* 1992) (Figure 7, a–c), but some spaced as far apart as with mature MAP2 (Figure 7, d–f). The analysis of microtubule spacing in the longitudinal sections revealed a mean ± SD for the three MAP2c-induced processes that was 35.19 ± 16.47 in proximal, 37.73 ± 25.67 in the middle portion, and 21.17 ± 14.88 in distal. The mean ± SD for three mature MAP2-induced processes was 90.71 ± 47.02 in proximal, 62.85 ± 18.01 in the middle portion of the process, and 50.90 ± 22.18 in distal. In one of these three processes, the spacing varied less along the process, 71.11 ± 21.80 in proximal, 61.35 ± 14.07 in the middle portion, and 52.5 ± 24.35 in distal, and the decrease of diameter was also less apparent (Figure 7, g–i).

The electron micrographs also suggested differences in the relative "straightness" or "waviness" of micro-

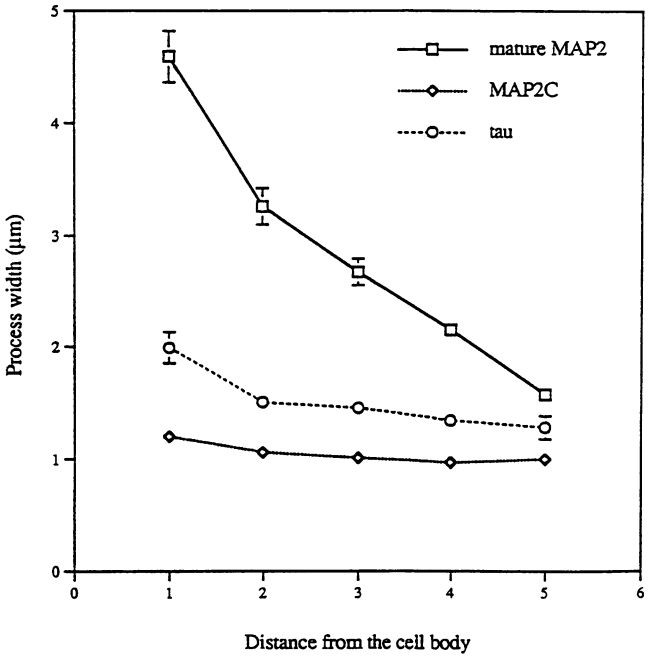

Figure 5. Graph showing the caliber of the processes induced by tau, mature MAP2, and MAP2c. Process width was measured as a function of distance from the cell body for each of the MAP constructs. The process diameter was measured at five points along the process. Mature MAP-2-induced processes presented the greatest tendency to taper.

tubules. Mature MAP2-induced microtubules showed the highest proportion of undulations along their length (Figure 7g). Given that all other parameters were the same for cells expressing different MAPs, these undulations were presumably a direct reflection of the stiffness of the microtubules.

DISCUSSION

We have used baculoviral expression to study the role of both MAP2c and mature MAP2 in cellular morphogenesis. As previously reported, the axonal MAP tau and both MAP2 isoforms induce process outgrowth in Sf9 cells. At identical molar ratios, MAP2c, mature MAP2, and tau give rise to a distinct pattern of process outgrowth. Sf9 cell expression suggests that MAPs function in sculpting unique process morphologies, a property that could not be predicted from the many in vitro studies (Drechsel *et al.*, 1992). How might MAPs give rise to unique types of processes? Since the MAP2 isoforms have identical microtubule-binding domains, and the related MAP, tau, has a homologous binding domain, the induction of unique types of processes may arise from their more variable projection domains. One known function of the projection domain is to set the spacing between microtubules (Chen *et al.*, 1992). Microtubules in Sf9 cells expressing mature MAP2 are spaced nearly three times as far apart as the microtubules in Sf9 cells expressing MAP2c. This constraint may then determine microtubule flexibility and possibly organelle translocation.

Our findings demonstrate that the determinants of microtubule spacing are more complex than simply setting a fixed distance with a specific MAP. In Sf9 cells expressing mature MAP2, the number of, and spacing between, microtubules decreased with distance from the cell body (Figure 6). Thus, the introduction of a single protein, mature MAP2, resulted in a variable microtubule organization that changed over the length of the process. Therefore, the primary sequence of the projection domain cannot be the sole determinant of spacing between neighboring microtubules. One explanation for these observations is that microtubules spacing is determined not only by the length of the projection domain, but also by its flexibility. For both MAPs and for the high and medium molecular weight neurofilament subunits, the phosphorylation state appears to regulate structural features of these proteins. Tau protein increased in rigidity when phosphorylated (Hagestedt *et al.*, 1989), and phosphorylation of MAPs does occur in Sf9 cells (Cheley *et al.*, 1992).

Differences in phosphorylation along an axon occur for tau (Mandel *et al.*, 1993) and neurofilaments (de Waegh *et al.*, 1992). Several studies have shown that the caliber of myelinated axons is regulated by neurofilament number (Hoffman *et al.*, 1987; Cleveland *et al.*, 1991). Local modulation of neurofilament phosphorylation by myelinating Schwann cells controls local changes in axonal caliber by controlling neurofilament packing density (de Waegh *et al.*, 1992). The carboxy-terminal domain of neurofilament subunits form a sidearm that contains several phosphorylation sites. Neurofilament sidearms, which are believed to be involved in mediating interactions between neurofilaments and neighboring structures, present a high surface charge under heavy phosphorylation, and are repelled from the surface of the neurofilaments and from neighboring neurofilaments resulting in greater distances between neurofilaments. A reduction of phosphorylation decreases the charge of the sidearms and consequently induces a closer packing of neurofilaments and smaller diameter. Phosphorylation of MAPs may induce similar repositioning of the MAP2 projection domain and/or may also affect the flexibility of the MAP2 projection domain. Consequently, a gradient of MAP2 phosphorylation may result in the tighter packing of microtubules distally.

Another possibility is that the differences in microtubule spacing may reflect a proximo-distal decreased concentration of mature MAP2 along the process. In vitro, it has been shown that MAP2 affects the packing density of sedimented microtubules whereas tau induces no change (Black, 1987; von Massow *et al.*, 1989).

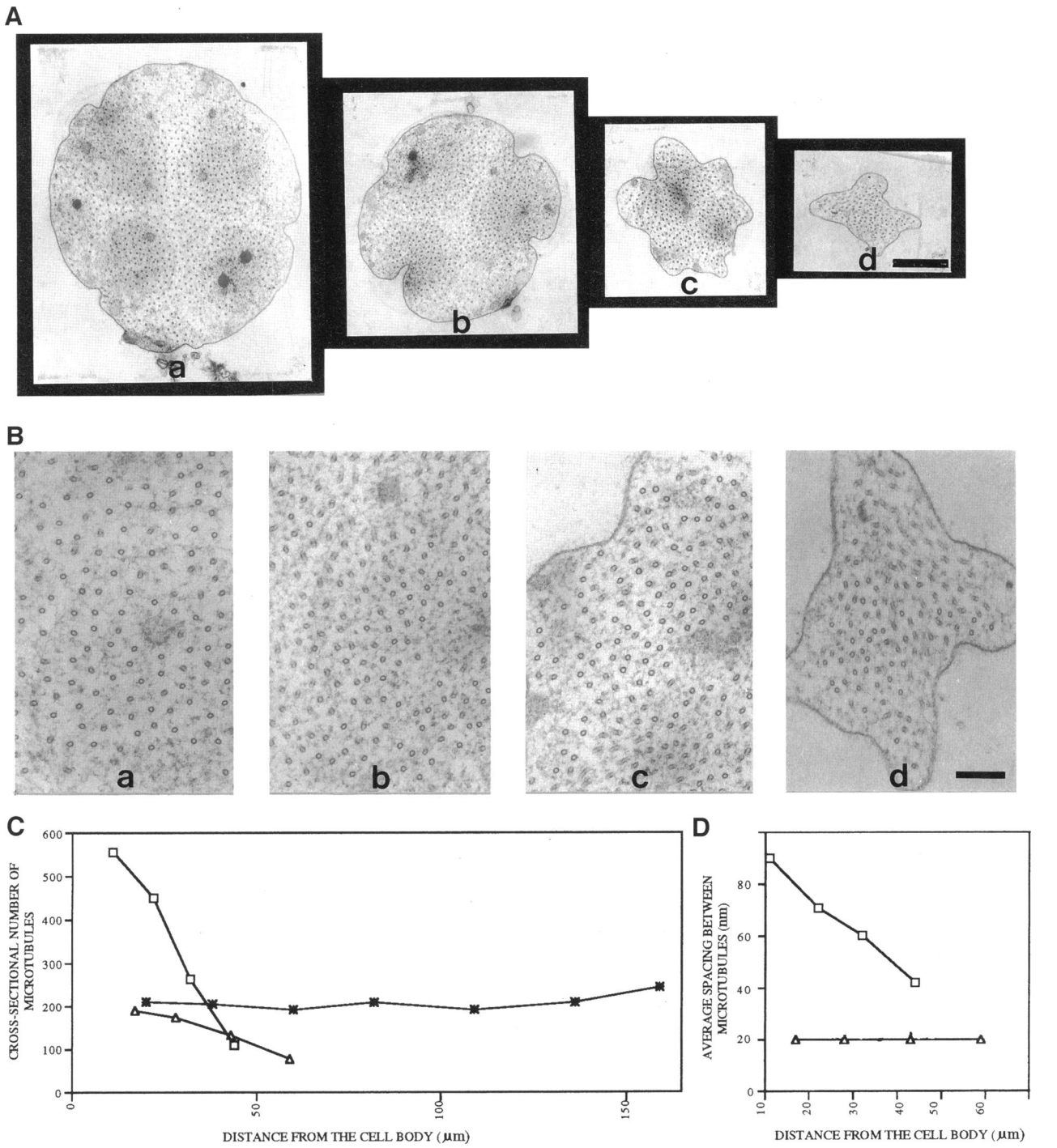

Figure 6. Analyses of microtubule organization along the length of a mature MAP2-induced process that decreases in caliber along its length. Cross-sections were taken at 10 μm apart along the process. In panel A, it is apparent that the number of microtubules (counted in panel C) decrease proximo-distally (a–d). Bar, 0.5 μm. At higher power (B) (bar, 0.2 μm), the spacing between microtubules appears to also decrease (measured in panel D). In panel C, the number of microtubules in each cross-section for mature MAP2 (square), MAP2c (star), and tau (triangle) was measured. In tau- and MAP2c-induced processes, the number of the microtubules are constant along the process whereas in MAP2-induced processes the number of microtubules decreases proximo-distally. In the same processes, the microtubule spacing (wall-to-wall) decreases in mature MAP2-induced process and remains constant in tau process (D).

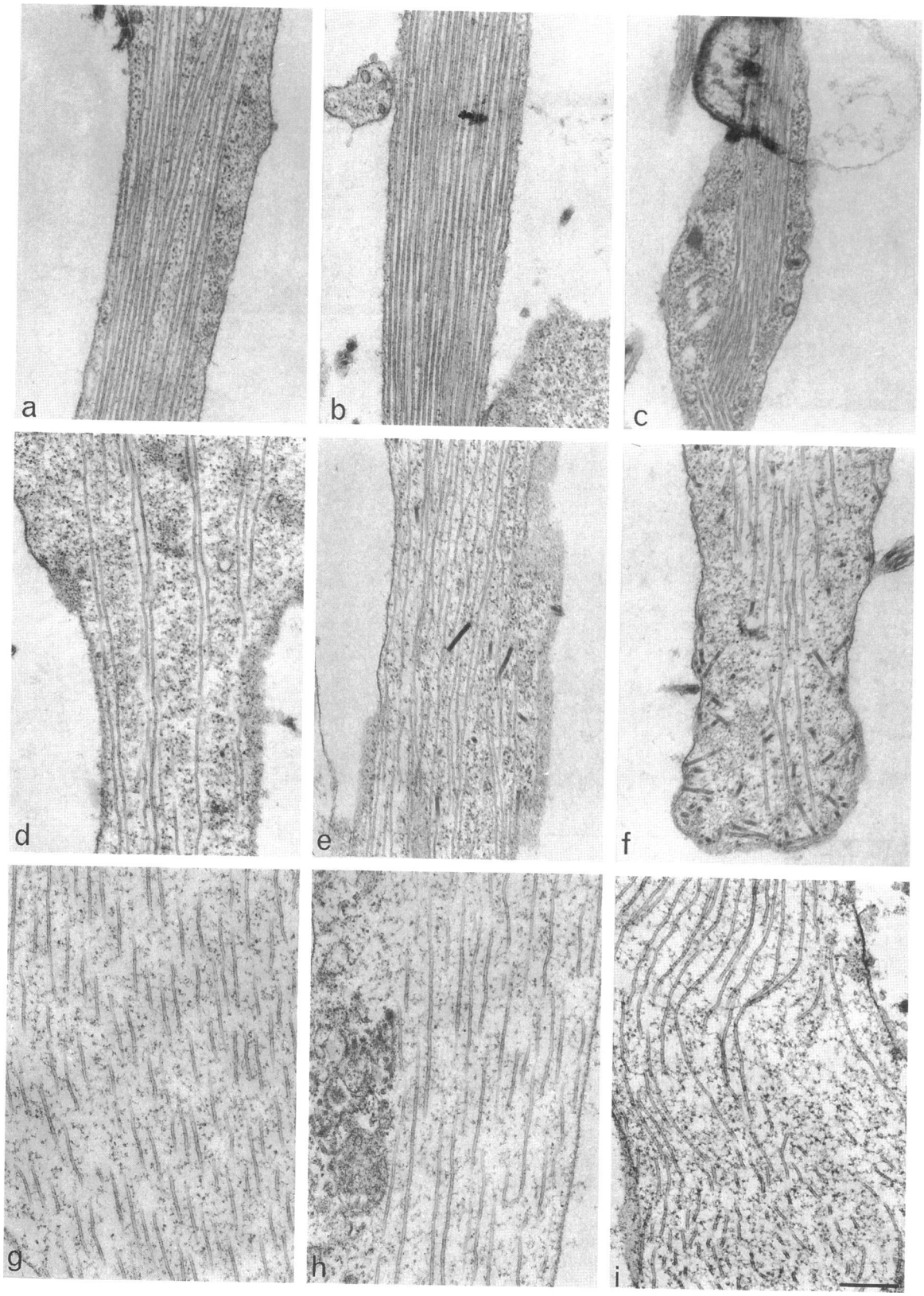

Figure 7.

These data showed that in microtubules containing tubulin and equal amounts of tau or MAP2, the MAP2-containing microtubules are farther apart than the tau-containing microtubules. Moreover, the spacing between MAP2-containing microtubules increases proportionally to an increase in MAP2 concentration, but an increase in tau concentration does not affect the microtubule spacing. This could explain why we observe a fairly consistent spacing in tau-induced processes even if the amount of tau may change over the length of the process. It is unclear whether or not changes in microtubule spacing occur along the length of bona fide dendrites. In one serial section analysis of the dendrites of cultured hippocampal neurons, we found that microtubules near the distal tip of the dendrite were more closely spaced than microtubules in more proximal regions of the dendrite (Sharp and Baas, unpublished data). Additional studies on more of these dendrites as well as the dendrites from other types of neurons will be required to determine whether progressively spaced microtubules consistently characterize bona fide dendrites. At present, we cannot dismiss the possibility that in the Sf9 system, differences in microtubule spacing are the result and not the cause of taper. An additional factor that also contributes to a proximo-distal decrease of MAP2-process caliber is the decreased number of microtubules along the process. It has been reported that the decreased number of microtubules per cross-sectional area of dendrite is concomitant with a reduction of caliber proximo-distally (Hillman, 1988). This suggests that the number of microtubules and spacing between these microtubules both regulate the diameter of a process.

Electron microscopy reveals notable differences in the straightness of the microtubule-induced MAP2 isoforms. The microtubules containing MAP-2c, similar to those containing tau, were generally straight but showed occasional contours. In contrast, the microtubules containing mature MAP-2 were significantly more wavy. In previous work, it was suggested that the stiffness resulted from coupling of the adjacent tubulin subunits to one another by the repeated tubulin-binding motifs contained in the microtubule-binding domain (Matus, 1994). Our studies do not test whether the microtubule binding domain is the more important part of the MAP-2 molecule with regard to conferring stiffness onto microtubules. However, comparison of MAP2c and mature MAP-2 reveal that the elongated projection domain of mature MAP2 may contribute to define the stiffness of the microtubule. The binding domain probably does confer stiffness to the microtubule as suggested by Matus (1994), but the elongated projection domain of mature MAP-2 may modulate this effect. In fact, it has been shown that the regions adjacent to the microtubule-binding domain exert modulatory effects on microtubule binding activity (Brandt and Lee, 1993a,b). The inherent flexibility of MAP2 could also influence the flexibility conferred to microtubules. Phosphorylation of tau increases its rigidity (Hagestedt *et al.*, 1989) and this modification could alter the flexibility of microtubules.

In contrast to cells expressing mature MAP2, which have as their salient feature a single tapered process, cells expressing MAP2c have multiple thin processes. These very different patterns of process outgrowth raise the question of how cells regulate process number. One leading idea is that process emergence from a particular site on the cell surface requires an interruption of the integrity of the cortical actin cytoskeleton. Microtubule assembly alone is not sufficient for MAPs to induce process outgrowth in Sf9 cells; cortical actin also influences the phenotype induced by MAPs. There is evidence that actin acts as a barrier to influence microtubule organization in Sf9 cells. After treatment with cytochalasin, tau-expressing cells shift from single to multiple processes and increased the rate of process elongation (Knowles *et al.*, 1994). In MAP2c-transfected mammalian cells, depolymerization of actin filaments results in the emergence of multiple microtubule-bearing processes (Edson *et al.*, 1993).

The expression of the MAP2c-like construct, FS, in which 109 amino acids had been deleted from the region that flanks the microtubule-binding domain, leads to the induction of an intermediate number of processes with 23% of the cells bearing more than three processes compared with 60% of the MAP2c-expressing cells and 10% of the mature MAP2-expressing cells (Leclerc *et al.*, 1993). This demonstrates that the flanking region to the microtubule-binding domain exerts a modulatory effects on the cellular activity of MAP2c. This region has been shown to be necessary to induce microtubule bundling in MAP2c-transfected COS cells (Umeyama *et al.*, 1993). This region is present in mature MAP2 that induces a single process, suggesting that the additional sequence contained in the projection domain of mature MAP2 regulates the effects exerted by the flanking region to the microtubule-binding domain. At any stage of the infection, approximately 27% of the MAP2c-expressing cells develop a single process. In these cells, the multiple bundles of microtubule form a tight bundle at the

Figure 7 (cont). Electron micrographs illustrating longitudinal sections of MAP2c and mature MAP2-induced processes. In some cases, the microtubule spacing in MAP2c-induced processes is similar to tau-induced processes with an average microtubule spacing of 30.95 ± 13.03 in proximal (a), 27.86 ± 9.90 in the middle portion (b), and 11.29 ± 10.54 in distal (c). In other cases, the microtubules are farther apart, with an average spacing of 38.32 ± 17.12 in proximal (d), 35.41 ± 23.70 in the middle portion (e), and 32.69 ± 10.07 in distal (f). The tapering of the mature MAP2-induced processes corresponds to the decrease of microtubule spacing proximo-distally (g–i). Bar, .25 μm.

emergence site of the process. This could signify that the ability of MAP2c to rearrange the Sf9 cell cytoskeleton is a function of time in the cell cycle.

These results provide evidence that MAPs have the capacity to induce the elaboration of processes with distinct shapes and suggest a developmental schema of neuronal process maturation in culture. Initially, multiple minor neurites extend from a rounded cell, a phenomenon that can be inhibited with MAP2 antisense oligonucleotide suppression (Caceres *et al.*, 1992) and perhaps effectuated by MAP2c. Later one neurite grows rapidly and becomes the axon, a phenomenon that may be mediated by the onset of tau expression (Caceres and Kosik, 1990). Finally the remaining minor neurites thicken in their proximal segments and begin to taper as they differentiate into dendrites. This event may be mediated by isoform switching to mature MAP2. Later in development, the invasion of neurofilaments, particularly in axons, increases the volume and sets the caliber of processes (Hoffman *et al.*, 1987). In this manner, the developmental regulation of MAPs and other cytoskeletal elements contribute to the staged morphological changes characteristic of neuronal development.

ACKNOWLEDGMENTS

We thank Nicholas Cowan for providing the mature MAP2 cDNA, and Lester Binder for providing antibody AP18. We acknowledge the excellent technical help of Tom Pienkowski and Kelly Cimbalnik for the electron microscopy. We also thank Gaston Lambert for the photographic work. This work was supported by National Institutes of Health grants NS-29031 and AG-06601 to K.S.K., and NS-28785 and NSF IBN-9209939 to P.W.B., who is also the recipient of a Research Career Development Award from the NIH. N.L. is supported by a Canadian Medical Research Council Fellowship.

REFERENCES

Baas, P.W., Deitch, J.S., Black, M.M., and Banker, G.A. (1988). Polarity orientation of microtubules in hippocampal neurons: uniformity in the axon and nonuniformity in the dendrite. Proc. Natl. Acad. Sci. USA *85*, 8335–8339.

Baas, P.W., and Heidemann, S.R. (1986). Microtubule reassembly from nucleating fragments during the regrowth of amputated neurites. J. Cell Biol. *21*, 397–427.

Baas, P.W., Pienkowski, T.P., and Kosik, K.S. (1991). Processes induced by tau expression in Sf9 cells have an axon-like microtubule organization. J. Cell Biol. *115*, 1333–1344.

Baas, P.W., Sinclair, G.I., and Heidemann, S.R. (1987). Role of microtubules in the cytoplasmic compartmentation of neurons. Brain Res. *420*, 73–81.

Banker, G., and Goslin, K. (1990). Culturing Nerve Cells, ed. C.F. Stevens, Cambridge, MA: The MIT Press.

Bartlett, W.P., and Banker, G.A. (1984). An electron microscopic study of the development of axons and dendrites by hippocampal neurons in culture. I. Cells which develop without intercellular contacts. J. Neurosci. *4*, 1944–1953.

Black, M.M. (1987). Comparison of the effects of microtubule-associated protein 2 and tau on the packing density of in vitro-assembled microtubules. Proc. Natl. Acad. Sci. USA *84*, 7783–7787.

Brandt, R., and Lee, G. (1993a). Functional organization of microtubule-associated protein tau. J. Biol. Chem. *268*, 3414–3419.

Brandt, R., and Lee, G. (1993b). The balance between tau protein's microtubule growth and nucleation activities: implications for the formation of axonal microtubules. J. Neurochem. *61*, 997-1005.

Burton, P.R., and Paige, J.L. (1981). Polarity of axoplasmic microtubules in the olfactory nerve of the frog. Proc. Natl. Acad. Sci. USA *78*, 3269–3273.

Caceres, A., and Kosik, K.S. (1990). Inhibition of neurite polarity by tau antisense oligonucleotides in primary cerebellar neurons. Nature *343*, 461–463.

Caceres, A., Mautino, J., and Kosik, K.S. (1992). Suppression of MAP2 in cultured cerebellar macroneurons inhibits minor neurite formation. Neuron *9*, 607–618.

Caceres, A., Potrebic, S., and Kosik, K. (1991). The effect of tau antisense oligonucleotides on neurite formation of cultured cerebellar macroneurons. J. Neurosci. *11*, 1515–1523.

Chen, J., Kanai, Y., Cowan, N.J., and Hirokawa, N. (1992). Projection domains of MAP2 and tau determine the spacings between microtubules in dendrites and axons. Nature *360*, 674–677.

Cheley, S., Kosik, K.S., Paskevich, P., Bakalis, S., and Bayley, H. (1992). Phosphorylated baculovirus p10 is a heat-stable microtubule-associated protein associated with process formation in Sf9 cells. J. Cell Sci. *102*, 739–752.

Cleveland, D., Monteiro, M.J., Wong, P.C., Gill, S.R., Geirhart, J.D., and Hoffman, P.N. (1991). Involvement of neurofilaments in the radial growth of axons. J. Cell Sci. Suppl. *15*, 85–95.

de Waegh, S.M., Lee, V.M.-Y., and Brady, S.T. (1992). Local modulation of neurofilament phosphorylation, axonal caliber, and slow axonal transport by myelinating Schwann cells. Cell *68*, 451–463.

Drechsel, D.N., Hyman, A.A., Cobb, M.H., and Kirschner, M.W. (1992). Modulation of the dynamic instability of tubulin assembly by the microtubule-associated protein tau. Mol. Biol. Cell *3*, 1141–1154.

Edson, K., Weisshaar, B., and Matus, A. (1993). Actin depolymerization induces process formation on MAP2-transfected non-neuronal cells. Development *117*, 689–700.

Fung, M.-C., Chiu, K.Y.M., Weber, T., Chang, T.W., and Chang, N.T. (1988). Detection and purification of a recombinant human B lymphotropic virus (HHV-6) in the baculovirus expression system by limiting dilution and DNA dot-blot hybridization. J. Virol. Methods *19*, 33–42.

Garner, C.C., and Matus, A. (1988). Different forms of microtubule-associated protein 2 are encoded by separate mRNA transcripts. J. Cell Biol. *106*, 779–783.

Hagestedt, T., Lichenberg, B., Wille, H., Mandelkow, E.M., and Mandelkow, E. (1989). Tau protein becomes long and stiff upon phosphorylation: correlation between paracrystalline structure and degree of phosphorylation. J. Cell Biol. *109*, 1643–1651.

Heidemann, S.R., Landers, J.M., and Hamborg, M.A. (1981). Polarity orientation of axonal microtubules. J. Cell Biol. *91*, 661–665.

Hillman, D.E. (1988). Parameters of dendritic shape and substructure: intrinsic and extrinsic determinants? In: Intrinsic Determinants of Neuronal Form and Function. ed. R.J. Lasek and M.M. Black, New York: Alan R. Liss, 83–113.

Hoffman, P.N., Cleveland, D.W., Griffin, J.W., Landes, P.W., Cowan, N.J., and Price, D.L. (1987). Neurofilament gene expression: a major

determinant of axonal caliber. Proc. Natl. Acad. Sci. USA *84*, 3472–3476.

Kindler, S., Schulz, B., Goedert, M., and Garner, C.C. (1990). Molecular structure of microtubule-associated protein 2b and 2c from rat brain. J. Biol. Chem. *265*, 19679–19684.

Kitts, P.A., Ayres, M.D., and Possee, R.D. (1990). Linearization of baculovirus DNA enhances the recovery of recombinant virus expression vectors. Nucleic Acids Res. *18*, 5667–5672.

Knops, J., Kosik, K.S., Lee, G., Pardee, J.D., Cohen-Gould, L., and McConlogue, L. (1991). Overexpression of tau in a nonneuronal cell induces long cellular processes. J. Cell Biol. *114*, 725–733.

Knowles, R., Leclerc, N., and Kosik, K.S. (1994). Organization of actin and microtubules during process formation in tau-expressing Sf9 cells. Cell Motil. Cytoskeleton *28*, 256–264.

Kosik, K.S., and Caceres, A. (1991). Tau protein and the establishment of an axonal morphology. J. Cell Sci. Suppl. *15*, 69–74.

Kosik, K.S., and McConlogue, L. (1994). Microtubule-associated protein function: lessons from expression in *Spodoptera frugiperda* cells. Cell Motil. Cytoskeleton *28*, 195–198.

Kosik, K.S., Orecchio, L.D., Binder, L.I., Trojanowski, J., Lee, V., and Lee, G. (1988). Epitopes that span the tau molecule are shared with paired helical filaments. Neuron *1*, 817–825.

Leclerc, N., Kosik, K.S., Cowan, N., Pienkowski, T.P., and Baas, P.W. (1993). Process formation in Sf9 cells induced by the expression of a microtubule-associated protein 2C-like construct. Proc. Natl. Acad. Sci. USA *90*, 6223–6227.

Lewis, S.A., Wang, D., and Cowan, N.J. (1988). Microtubule-associated protein MAP2 shares a microtubule-binding motif with tau protein. Science *242*, 936–939.

Ludin, B., and Matus, A. (1993). The neuronal cytoskeleton and its role in axonal and dendritic plasticity. Hippocampus *3*, 61–72.

Mandel, J.W., Benson, D.L., and Banker, G.A. (1993). A spatial gradient of tau protein phosphorylation in nascent axons. Soc. Neurosci. *19*, 1082 (Abstract 448.9).

Matus, A. (1994). Stiff microtubules and neuronal morphology. Trends Neurosci. *17*, 19–22.

Papandrikopoulou, A., Doll, T., Tucker, R.P., Garner, C.C., and Matus, A. (1989). Embryonic MAP2 lacks the cross-linking sidearm sequences and dendritic targeting signal of adult MAP2. Nature *340*, 650–652.

Sharma, N., Kress, Y., and Shafit-Zagardo, B. (1994). Antisense MAP2 oligonucleotides induce changes in microtubule assembly and neuritic elongation in pre-existing neurites of rat cortical neurons. Cell Motil. Cytoskeleton *27*, 234–247.

Summers, M.D., and Smith, G.E. (1987). A Manual of Methods for Baculovirus Vectors and Insect Cell Culture Procedures, Bulletin No. 1555, College Station, TX: Texas Agricultural Experiment Station and Texas A&M University.

Towbin, H., Staehelin, T., and Gordon, J. (1979). Electrophoretic transfer of proteins from polyacrylamide gels to nitrocellulose sheets: procedure and some application. Proc. Natl. Acad. Sci. USA *76*, 4350–4353.

Tucker, R.P., Binder, L.I., Viereck, C., Hemmings, B.A., and Matus, A. (1988). The sequential appearance of low- and high-molecular weight forms of MAP2 in the developing cerebellum. J. Neurosci. *12*, 4503–4512.

Umeyama, T., Okabe, S., Kanai, Y., and Hirokawa, N. (1993). Dynamics of microtubules bundled by microtubule-associated protein 2C (MAP2C). J. Cell Biol. *120*, 451–465.

von Massow, A., Mandelkow, E.-M., and Mandelkow, E. (1989). Interaction between kinesin, microtubules, and microtubule-associated protein 2. Cell Motil Cytoskeleton *14*, 562–571.